Pressure suppression of the excitonic insulator state in Ta₂NiSe₅ observed by optical conductivity

H. Okamura [1,*] T. Mizokawa,[2] K. Miki,[1] Y. Matsui,[1] N. Noguchi,[1] N. Katayama,[3] H. Sawa,[3] M. Nohara,[4]
Y. Lu,[5] H. Takagi,[6,7] Y. Ikemoto,[8] and T. Moriwaki[8]

[1]*Department of Applied Chemistry, Tokushima University, Tokushima 770-8506, Japan*
[2]*Department of Applied Physics, Waseda University, Tokyo 169-8555, Japan*
[3]*Department of Applied Physics, Nagoya University, Nagoya 464-8603, Japan*
[4]*Department of Quantum Matter, Hiroshima University, Higashi-Hiroshima 739-8503, Japan*
[5]*College of Materials Science and Engineering, National Engineering Research Center for Magnesium Alloys,*
Chongqing University, Chongqing 400044, China
[6]*Department of Physics, University of Tokyo, Tokyo 113-0013, Japan*
[7]*Max Planck Institute for Solid State Research, 70569 Stuttgart, Germany*
[8]*Japan Synchrotron Radiation Research Institute, Sayo 679-5198, Japan*

The layered chalcogenide Ta₂NiSe₅ has recently attracted much interest as a strong candidate for a long-sought excitonic insulator (EI). Since the physical properties of an EI are expected to depend sensitively on the external pressure (P), it is important to clarify the P evolution of a microscopic electronic state in Ta₂NiSe₅. Here we report the optical conductivity [$\sigma(\omega)$] of Ta₂NiSe₅ measured at high P to 10 GPa and at low temperatures to 8 K. With cooling at $P = 0$, $\sigma(\omega)$ develops an energy gap of about 0.17 eV and a pronounced excitonic peak at 0.38 eV as reported previously. With increasing P, the energy gap becomes narrower and the excitonic peak is diminished. Above a structural transition at $P_s \simeq 3$ GPa, the energy gap becomes partially filled, indicating that Ta₂NiSe₅ is a semimetal after the EI state is suppressed by P. At higher P, $\sigma(\omega)$ exhibits metallic characteristics with no energy gap. The detailed P evolution of the energy gap and $\sigma(\omega)$ is presented, and discussed mainly in terms of a weakening of excitonic correlation with P.

I. INTRODUCTION

An excitonic insulator (EI) is an unconventional insulator in which the attractive correlation between electrons and holes results in a collective condensation of electron-hole (*e-h*) pairs (excitons) and an energy gap at the Fermi level (E_F). EIs were first predicted theoretically in the 1960s [1] with a phase diagram schematically shown in Fig. 1. The starting material for an EI can be either a semimetal ($E_g < 0$) or a semiconductor ($E_g > 0$), where E_g indicates the one-particle band gap in the absence of *e-h* correlation. An EI state is expected in the vicinity of $E_g = 0$ below the transition temperature T_c if the exciton binding energy E_b is larger than $|E_g|$. Another feature of the EI is a characteristic flattening of the bands as illustrated in Fig. 1.

Despite the theoretical interest in EIs, only a few compounds had been considered as candidates for EIs, including TmSe$_{1-x}$Te$_x$ [2] and 1T-TiSe₂ [3]. In 2009, Wakisaka *et al.* [4] suggested that Ta₂NiSe₅ should be an EI on the basis of angle-resolved photoemission spectroscopy (ARPES) data. Ta₂NiSe₅ has a layered crystal structure, and exhibits a structural phase transition at $T_c = 328$ K, where the crystal symmetry changes from orthorhombic to monoclinic with decreasing temperature (T) [5,6]. Below T_c, the resistivity increases rapidly with cooling, indicating an energy gap of

about 0.2 eV [6]. The ARPES study at low T found an unusually flat dispersion at the top of the valence band, which was regarded as strong evidence for an EI [4]. Further ARPES studies [7] and band calculations [7,8] indicated that the flat-band feature persisted even above T_c, and suggested the low-T phase of Ta₂NiSe₅ to be an EI in the strong-coupling regime caused by a condensation of preformed excitons [7,8]. It was pointed out that above T_c the hybridization between the Ta 5d conduction band and the Ni 3d valence band at the Γ point should be forbidden by symmetry. It was also suggested that the structural change below T_c was mainly driven by the exciton condensation, rather than by a structural instability due to electron-lattice (*e-l*) coupling [8]. Lu *et al.* [9] reported transport and optical data of Ta₂Ni(Se,S)₅ and Ta₂Ni(Se,Te)₅, where the chemical substitution and external pressure were used to control E_g of Ta₂NiSe₅. The optical conductivity [$\sigma(\omega)$] of Ta₂NiSe₅ at low T clearly exhibited a pronounced peak of excitonic origin at about 0.4 eV and an energy gap of about 0.16 eV. An experimental phase diagram of Ta₂NiSe₅ was constructed from the transport data, which was indeed consistent with the predicted one depicted in Fig. 1 and strongly suggested Ta₂NiSe₅ to be an EI [9]. Detailed $\sigma(\omega)$ data [10] were analyzed by a theoretical study [11], which again suggested that Ta₂NiSe₅ should be an EI in the strong-coupling regime below T_c, and it should be a semiconductor ($E_g > 0$) above T_c [11].

Many more works on Ta₂NiSe₅ have also been reported, including ARPES [12–21], optical conductivity [22,23], Raman
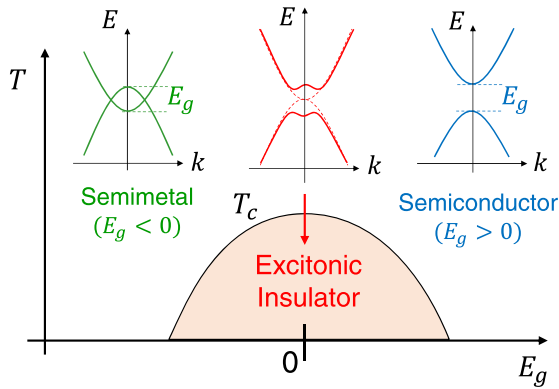
---

*ho@tokushima-u.ac.jp

FIG. 1. Schematic phase diagram of EI in terms of the temperature (T) and the one-particle band gap in the absence of *e-h* correlation (E_g). Positive and negative values of E_g correspond to semiconducting and semimetallic states, respectively. An EI state is expected in the vicinity of $E_g = 0$ below the transition temperature (T_c), with a characteristic flattening of the band edges as indicated.

FIG. 2. Temperature-pressure (T-P) phase diagram of Ta_2NiSe_5 after Matsubayashi *et al.* [23]. T_c, T^*, and P_s indicate the structural transition temperatures and pressure, and T_{sc} the superconducting transition temperature. The green arrows and dots indicate the (P, T) paths and points where $\sigma(\omega)$ was measured in this work.

scattering [24–28], ultrafast laser spectroscopy [29–31], resonant inelastic x-ray scattering [32,33], high pressure studies [23,26,34], scanning tunneling spectroscopy [35], and theoretical analyses [20,36,37]. While many of these works support that the transition at T_c is driven by exciton condensation, some of them question such scenario [20,33,36]. For example, a semimetallic ($E_g < 0$) band dispersion around E_F has been reported by an ARPES study above T_c [20]. Theoretically, it has been shown that a flat valence band may be obtained by a band calculation without *e-h* correlation [20], and that there can be a sizable (~ 0.1 eV) hybridization with the mirror symmetry breaking below T_c but without *e-h* correlation [36].

Following the above development, it is important to carefully evaluate the effects of both the *e-h* correlation and the *e-l* coupling in Ta_2NiSe_5. An important aspect is the response of Ta_2NiSe_5 to changes in the ratio E_b/E_g, since the physical properties of EIs should sensitively depend on E_b/E_g. In this regard, photoexcited experiments, which are probed by either ARPES [12–17] or laser [29–31], have the advantage of being able to tune the carrier density, and hence to control E_b through the Coulomb screening of *e-h* attraction. In fact, photoinduced gap closing and semimetallic states in Ta_2NiSe_5 have been observed and analyzed [12–17,31]. Another effective way of tuning an EI state is the application of external pressure (P) [9,23,26,34], since an applied pressure usually broadens the conduction and valence bands, and increases (reduces) their overlap (separation). Detailed high-P studies [23,34] have been performed on the crystal structure, resistivity (ρ), Hall coefficient, and $\sigma(\omega)$ of Ta_2NiSe_5. They revealed a rich P-T phase diagram of Ta_2NiSe_5 as depicted in Fig. 2. Above the first-order structural transition at $P_s \simeq 3$ GPa, the *ac* plane becomes flatter with less rippling of the *ac* plane along the *c* axis [23,34]. $\rho(T)$ is reduced with increasing P, showing a crossover from semiconducting T dependence below P_s to a completely metallic one well above P_s, with a quite large and dramatic change of $\rho(T)$ around P_s. A superconductivity with $T_c = 2$ K appears at about 8 GPa. Above P_s, from $\rho(T)$ and $\sigma(\omega)$ data, it has been shown that Ta_2NiSe_5 is a semimetal with a partial energy gap, in contrast to the full
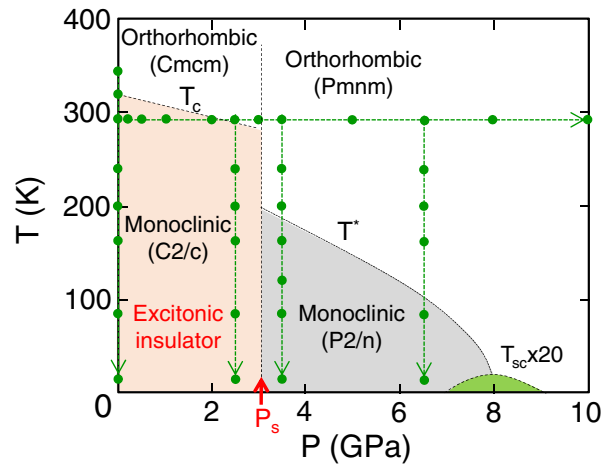
energy gap below P_s. It has been suggested that the electronic transition at T^* to the low-T semimetallic state is caused by *e-l* coupling, while that at T_c below P_s is caused by both excitonic correlation and *e-l* coupling [23].

In this paper, we present a full account of the $\sigma(\omega)$ and reflectance data of Ta_2NiSe_5 at high P and low T, which have been obtained at the (P, T) points indicated in Fig. 2. The data reveal how the well-developed energy gap and excitonic peak at $P = 0$, which have been taken as evidence for an EI, are suppressed as the applied pressure reduces the excitonic correlation. We have also measured the optical spectra at $P = 0$, since they are very important in analyzing the high-P data. Nevertheless, full details of our $P = 0$ data are shown in the Supplemental Material [38], since the $P = 0$ spectra have already been reported [10,22] and since our $P = 0$ results are similar to the reported ones. Below, selected $P = 0$ spectra from our results are shown in comparison with the high-P data.

II. EXPERIMENTAL DETAILS

The samples of Ta_2NiSe_5 used were single crystals grown with the chemical vapor transport method as reported previously [9]. Reflectance spectra of a sample at high P were measured using a diamond-anvil cell (DAC) [39]. Type-IIa diamond anvils with a 0.8-mm culet diameter and a stainless-steel gasket were used to seal the sample with KBr as the pressure transmitting medium. An as-grown surface of a sample was directly attached on the culet surface of the diamond anvil, and the reflectance at the sample/diamond interface [$R_d(\omega)$] was measured. A gold film was also sealed with the sample as the reference of reflectance. The pressure in the DAC was measured with the ruby fluorescence method [40]. $R_d(\omega)$ at high P and low T were measured at photon energies between 0.025 and 1.1 eV, using synchrotron radiation as a bright infrared source [41] at the beamline BL43IR of SPring-8 [42]. The measured $R_d(\omega)$ spectra below 1.1 eV
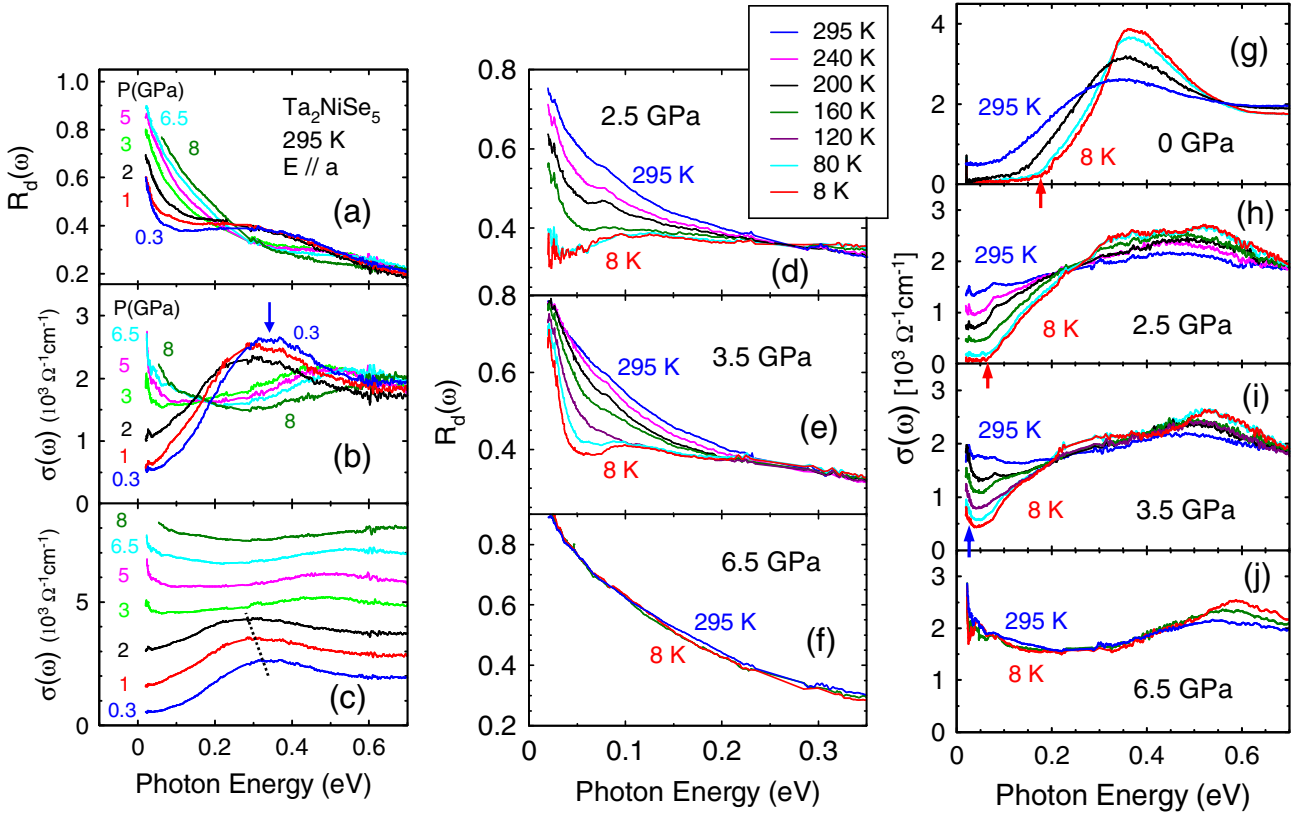
FIG. 3. (a) Optical reflectance [$R_d(\omega)$] and (b),(c) conductivity [$\sigma(\omega)$] of Ta$_2$NiSe$_5$ at 295 K under high pressure (P). $R_d(\omega)$ in the 0.235–0.285 eV range has been interpolated by a straight line since it could not be measured well due to strong absorption by diamond [39]. The arrow in (b) indicates the excitonic peak discussed in the text. In (c), the same spectra as those in (b) are vertically offset, and the broken line emphasizes the shifts and strong suppression of the excitonic peak observed near P_s = 3 GPa. (d)–(f) $R_d(\omega)$ of Ta$_2$NiSe$_5$ measured at P = 2.5, 3.5, and 6.5 GPa and at different temperatures. (g)–(j) $\sigma(\omega)$ of Ta$_2$NiSe$_5$ at P = 0, 2.5, 3.5, and 6.5 GPa and at low temperatures. The red vertical arrows in (g) and (h) indicate the onset of $\sigma(\omega)$, and the blue vertical arrow in (i) indicates the Drude component remaining at 8 K. The same temperature labels (the colors of the curves) apply in (d)–(f) and (g)–(j).

were connected to the $R_d(\omega)$ above 1.1 eV expected from the $R_0(\omega)$ measured at P = 0 and T = 295 K using the Kramers-Kronig (KK) analysis [43] and the refractive index of diamond (n_d = 2.4). Then the connected $R_d(\omega)$ spectra were used to obtain $\sigma(\omega)$ by a modified KK analysis method [44]. More details of the high-pressure infrared experiments using DAC have been reported elsewhere [39]. Experimental details about the P = 0 studies [45] are described in the Supplemental Material [38].

III. RESULTS AND DISCUSSION

In the crystal structure of Ta$_2$NiSe$_5$, the (-Ta-Se-) and (-Ni-Se-) chains extend along the a axis in the ac layers stacked along the b axis [5,6]. Therefore, characteristic optical responses of EIs are observed with $E \parallel a$ polarization where E is the electric field of the incident light. $R_d(\omega)$ and $\sigma(\omega)$ at high pressures and at 295 K with $E \parallel a$ are presented in Figs. 3(a)–3(c). At P = 0.3 GPa, $\sigma(\omega)$ is still similar to that at P = 0 [38], where the main features are the energy gap and the excitonic peak, the latter of which is indicated by the arrow in Fig. 3(b). Note that $\sigma(\omega)$ toward zero energy is not completely depleted yet unlike those at low T [see Fig. 3(g)] since there are thermally excited carriers at 295 K. With increasing P,

both $R_d(\omega)$ and $\sigma(\omega)$ below 0.2 eV exhibit large and rapid increases. In addition, the excitonic peak becomes broader and shifts to lower energy with P. Then, at 3 GPa and above, the excitonic peak has been strongly suppressed compared with that below 3 GPa. These results are more clearly seen in Fig. 3(c) where the $\sigma(\omega)$ spectra are vertically offset. The strong suppression of the excitonic peak near 3 GPa is almost coincident with the structural transition at P_s = 3 GPa, which is believed to be the boundary of the EI phase as shown in Fig. 2. Namely, the present result explicitly demonstrates that the excitonic peak is suppressed as the system goes out of the EI phase. In addition, the result that the excitonic peak becomes diminished with P even within the EI phase below P_s is also consistent with the fact that the system is approaching the EI phase boundary. As discussed in the Supplemental Material [38], the Raman spectra of Ta$_2$NiSe$_5$ at high P were also measured, using the same DAC and sample condition. The Raman spectra (Fig. S2) exhibit a sudden shift and disappearance of phonon peaks around 3 GPa, which should result from the first-order structural transition at P_s. This Raman result further supports that the observed spectral changes in $\sigma(\omega)$ indeed result from the structural transition at P_s. With further increasing P above 3 GPa, $\sigma(\omega)$ below 0.1 eV becomes higher with a rising (Drude) component toward zero energy. This

indicates that the electronic structures in Ta$_2$NiSe$_5$ become metallic at higher P, which is consistent with the $\rho(T)$ data measured in the same P range [23].

Temperature-dependent $R_d(\omega)$ spectra at $P = 2.5$, 3.5, and 6.5 GPa are indicated in Figs. 3(d)–3(f), and the corresponding $\sigma(\omega)$ spectra in Figs. 3(h)–3(j). First, note that the large T dependencies of $R_d(\omega)$ and $\sigma(\omega)$ observed at $P = 0$ are progressively reduced with increasing P. Accordingly, both the energy gap and excitonic peak at low T are progressively suppressed with P. At 2.5 GPa, $\sigma(\omega)$ develops a clear energy gap with cooling [Fig. 3(h)], but the onset of $\sigma(\omega)$ at 8 K is located at 0.062 eV, which is much smaller than that at $P = 0$ [Fig. 3(g)]. Namely, a clear energy gap still exists at $P = 2.5$ GPa, but its size has significantly been reduced from that at $P = 0$. At 3.5 GPa, $\sigma(\omega)$ below 0.2 eV is still strongly reduced with cooling, but unlike those at $P = 0$ and 2.5 GPa, it is not completely depleted even at 8 K. A rising component toward zero energy is observed even at 8 K, as indicated by the arrow in Fig. 3(i), which should be a Drude component due to free carriers. The thermal energy k_BT, where k_B is the Boltzmann constant, is about 0.7 meV at 8 K, while the tail of the Drude component at 8 K extends to much higher energy, ∼50 meV. Therefore, the electronic state at 3.5 GPa and 8 K is difficult to understand as a semiconductor with thermally excited free carriers. Instead, it should be a semimetal, where a low density of free carriers remains even at low T as shown by the weak Drude component. The appearance of a semimetallic state at high P is reasonable since an external P is expected to increase the bandwidths and drive the system toward the $E_g < 0$ side of Fig. 1. At 6.5 GPa, the spectra show only minor T dependencies, and $\sigma(\omega)$ below 0.4 eV is almost unchanged from 295 to 8 K. Clearly, at 6.5 GPa there is no energy gap in Ta$_2$NiSe$_5$ and its electronic structure is quite metallic.

To examine more closely the variations of energy gap with P and T, the low-energy portion of $\sigma(\omega)$ at $P = 0$ and 2.5 GPa are displayed in Figs. 4(a) and 4(b), respectively. The broken lines are extrapolations to the linear-in-energy portion in $\sigma(\omega)$. Their crossings with $\sigma(\omega) = 0$, marked with the vertical arrows, indicate the onset of $\sigma(\omega)$. Here we regard the onset energy as the gap size Δ, following a previous $\sigma(\omega)$ work on Ta$_2$NiSe$_5$ (Ref. [22]) and other optical studies on strongly correlated electron systems [46]. At $P = 0$ [Fig. 4(a)], the extrapolation crosses $\sigma(\omega) = 0$ at 295 K and below, but not at 320 K. Namely, the gap in $\sigma(\omega)$ becomes fully open at T between 320 and 295 K, which is reasonable since the gap formation starts below $T_c = 328$ K and the gap is not well developed yet at 320 K. The T dependence of the onset energy is plotted in Fig. 4(c). The result is similar to that previously reported by Ref. [22], which reported a T dependence of the form $\Delta(T) = \Delta(0)\{1 - (T/T_c)^\alpha\}$ with $\alpha = 2$. For comparison, in Fig. 4(c) we also plot this function with $T_c = 328$ K and $\alpha = 2$, 2.5, and 3. It is seen that the present data is close to $\alpha = 2.5$, but cannot be well described by a single exponent. At 2.5 GPa [Fig. 4(b)], the extrapolation crosses $\sigma(\omega) = 0$ at 160 K and below, but not at 200 K. Namely, the gap becomes fully open at T between 200 and 160 K, which is much lower than $T_c \simeq 290$ K at 2.5 GPa. This is in contrast to the $P = 0$ case above, where the gap in $\sigma(\omega)$ is already open at 295 K which is below but still close to $T_c = 328$ K. Namely, it seems that the P dependence of the energy gap in
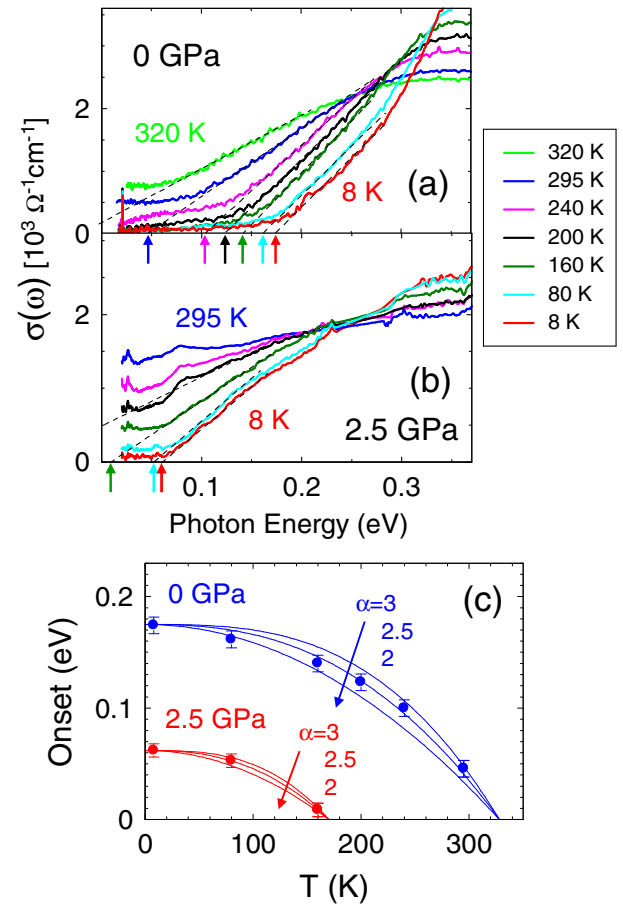

FIG. 4. Low-energy portion of $\sigma(\omega)$ in $E \parallel a$ polarization at (a) $P = 0$ and (b) $P = 2.5$ GPa. The broken lines indicate extrapolations to the linear-in-energy portion of the spectra, and the vertical arrows indicate the onset given by the crossing of the extrapolations with $\sigma(\omega) = 0$. (c) The onset energy in (a) and (b) plotted as a function of temperature (T). The curves indicate $\Delta(T) = \Delta(0)\{1 - (T/T_c)^\alpha\}$ with the indicated values of α. $\Delta(0) = 0.175$ eV and $T_c = 328$ K are used for $P = 0$, and $\Delta(0) = 0.062$ eV and $T_c = 170$ K for $P = 2.5$ GPa. The error bars indicate variations arising from how the extrapolations (straight lines) are drawn to the linear-in-energy portions of $\sigma(\omega)$ in (a) and (b).

$\sigma(\omega)$ is different from that of T_c. The T dependence of the onset at 2.5 GPa is also plotted in Fig. 4(c). It is similar to that at $P = 0$, but to fit with the form $\Delta(T) = \Delta(0)\{1 - (T/T_c)^\alpha\}$, $T_c \simeq 170$ K and $\alpha \simeq 2.5$ are required as shown by the red solid curves in Fig. 4(c). Note that the use of this functional form is only phenomenological, and not based on a microscopic theory for EIs. Nevertheless, the model is used here as a way of quantitatively expressing the observed T dependence of the energy gap, since this may be useful when the data need to be compared with theoretical predictions in the future. The much stronger suppression of energy gap by pressure than that of T_c will be discussed again later.

In the $\sigma(\omega)$ spectra at 2.5 GPa [Fig. 3(h)], a clear energy gap is still observed while the excitonic peak has been suppressed compared with that at $P = 0$. Namely, a well-developed energy gap still exists although a much weaker *e-h* correlation than that at $P = 0$ is suggested by the suppressed
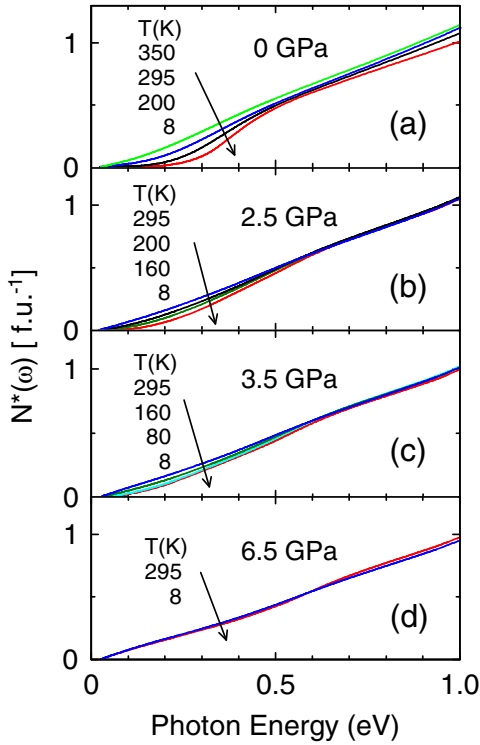
FIG. 5. Effective electron number $N^*(\omega)$ per formula unit (f.u.) of Ta$_2$NiSe$_5$, calculated with Eq. (1) and the measured $\sigma(\omega)$ spectra at different pressures and temperatures.

excitonic peak. This result may suggest a possibility that the energy gap at 2.5 GPa results not mainly from e-h correlation but from some other mechanism, which most likely is the hybridization effect as discussed in the Introduction. From the T dependence of the energy gap size in Fig. 4(c), however, it is unclear if there are qualitatively different characteristics between the gap at $P = 0$ and that at $P = 2.5$ GPa. In Ref. [23], the above possibility was not considered, and it was regarded that the EI phase should basically correspond to the low-P monoclinic phase below P_s, as indicated in Fig. 2. However, in the alternative possibility suggested above, the low-P monoclinic phase may not necessarily correspond to and may not completely overlap with the EI phase.

To analyze the spectral weight (SW) transfer in $\sigma(\omega)$ with P and T, the effective electron number $N^*(\omega)$ per formula unit (f.u.) of Ta$_2$NiSe$_5$, expressed as [43]

$$N^*(\omega) = \frac{n}{m^*}(\omega) = \frac{2m_0}{\pi e^2 N_0} \int_0^\omega \sigma(\omega')d\omega', \qquad (1)$$

is plotted in Fig. 5. Here, n, m^*, and e are the electron density, effective mass in units of the rest mass m_0, and the elementary charge. N_0 is the number of f.u.'s per unit volume, which was calculated using the high-P crystal structure data [34,47]. $N^*(\omega)$ can be regarded as the number of electrons that contribute to $\sigma(\omega)$ between 0 and ω, and therefore it directly reflects the SW transfer up to ω. At all P and T in Fig. 5, $N^*(\omega)$ at 1 eV is of the order of 1 f.u.$^{-1}$, which is reasonable compared with the total density of states within 1 eV from E_F given by band calculations [23]. At $P = 0$, $N^*(\omega)$ varies with T over a wide energy range. The $N^*(\omega)$ spectra at different

temperatures do not converge even at 1 eV, showing that the electronic structure reconstruction in the EI phase occurs over a wider energy scale than the gap size (0.17 eV) and the excitonic peak energy (0.4 eV). At 2.5 and 3.5 GPa, however, $N^*(\omega)$ varies with T only up to about 0.6 eV, indicating that the SW transfer is complete within 0.6 eV. At 6.5 GPa, $N^*(\omega)$ is almost independent of T. These results show that both the amount and energy range of the SW transfer are progressively suppressed by P, which is closely related with the suppression of the energy gap.

As discussed in the Introduction, it has been pointed out that the gap formation in Ta$_2$NiSe$_5$ below P_s may be partly due to e-l coupling, rather than being solely due to e-h (excitonic) correlation. If their relative contributions do not change with P, and if both the structural transition at T_c and the gap opening below T_c are driven by a common mechanism, then one would naively expect that Δ and T_c should have similar P dependencies. This is in contrast to the present results, in which the reduction of Δ by pressure is much greater than that of T_c (from $\Delta = 0.17$ eV and $T_c = 328$ K at $P = 0$ to $\Delta = 0.062$ eV and $T_c \simeq 290$ K at 2.5 GPa). Namely, in terms of the P dependence, Δ is not scaled with T_c. Interestingly, a pressure decoupling between electronic and structural transitions has been observed in BaFe$_2$As$_2$ [48], which is another pressure-induced superconductor. The present results for Ta$_2$NiSe$_5$ may suggest that, somehow, the e-h correlation is more responsible for the gap development below T_c, while the e-l coupling is more responsible for the structural transition at T_c. This would naturally lead to a stronger suppression of Δ than T_c by pressure, since the e-h correlation is likely more reduced by pressure than the e-l coupling as long as the structure does not change. An understanding of these P dependencies based on a specific microscopic model is beyond the scope of the present study. It is hoped that the effects of both the e-h correlation and the e-l coupling with symmetry breaking induced hybridization are both included in a microscopic model to understand the pressure evolution of electronic states in Ta$_2$NiSe$_5$.

IV. SUMMARY

$\sigma(\omega)$ spectra of Ta$_2$NiSe$_5$, a strong candidate for an EI, have been measured at high pressures and at low temperatures. A clear energy gap of about 0.17 eV and a marked excitonic peak at 0.38 eV at $P = 0$ are suppressed with increasing P, which is especially marked across the structural transition at $P_s = 3$ GPa. At 2.5 GPa ($<P_s$), the gap is still clearly open with a reduced size of 0.062 eV, but at 3.5 GPa ($>P_s$), the gap is partially filled, indicating that the ground state above P_s is semimetallic. Detailed T dependence of the energy gap is analyzed and compared between $P = 0$ and 2.5 GPa, but it is unclear whether the characteristics of the gap change from $P = 0$ to 2.5 GPa. At 6.5 GPa, $\sigma(\omega)$ shows very metallic characteristics with no energy gap. These results have been discussed in terms of a progressive weakening of excitonic correlation with pressure. Also, it is noted that the reduction of energy gap with pressure is much greater than that of T_c. This result may suggest that the relative importance of e-h correlation and e-l coupling in the gap formation changes with pressure.

[1] For review on the early development, see, for example, B. I. Halperin and T. M. Rice, Possible anomalies at a semimetal-semiconductor transistion, Rev. Mod. Phys. **40**, 755 (1968).

[2] B. Bucher, P. Steriner, and P. Wachter, Excitonic Insulator Phase in $TmSe_{0.45}Te_{0.55}$, Phys. Rev. Lett. **67**, 2717 (1991).

[3] H. Cercellier, C. Monney, F. Clerc, C. Battaglia, L. Despont, M. G. Garnier, H. Beck, P. Aebi, L. Patthey, H. Berger, and L. Forro, Evidence for an Excitonic Insulator Phase in $1T$-$TiSe_2$, Phys. Rev. Lett. **99**, 146403 (2007).

[4] Y. Wakisaka, T. Sudayama, K. Takubo, T. Mizokawa, M. Arita, H. Namatame, M. Taniguchi, N. Katayama, M. Nohara and H. Takagi, Excitonic Insulator State in Ta_2NiSe_5 Probed by Photoemission Spectroscopy, Phys. Rev. Lett. **103**, 026402 (2009).

[5] S. Sunshine and J. Ibers, Structure and physical properties of the new layered ternary chalcogenides tantalum nickel sulfide (Ta_2NiS_5) and tantalum nickel selenide (Ta_2NiSe_5), Inorg. Chem. **24**, 3611 (1985).

[6] F. J. Di Salvo, C. Chen, R. Fleming, J. Waszczak, R. Dun, S. Sunshine, and J. Ibers, Physical and structural properties of the new layered compounds Ta_2NiS_5 and Ta_2NiSe_5, J. Less-Common Met. **116**, 51 (1986).

[7] K. Seki, Y. Wakisaka, T. Kaneko, T. Toriyama, T. Konishi, T. Sudayama, N. L. Saini, M. Arita, H. Namatame, M. Taniguchi, N. Katayama, M. Nohara, H. Takagi, T. Mizokawa, and Y. Ohta, Excitonic Bose-Einstein condensation in Ta_2NiSe_5 above room temperature, Phys. Rev. B **90**, 155116 (2014).

[8] T. Kaneko, T. Toriyama, T. Konishi, and Y. Ohta, Orthorhombic-to-monoclinic phase transition of Ta_2NiSe_5 induced by the Bose-Einstein condensation of excitons, Phys. Rev. B **87**, 035121 (2013).

[9] Y. F. Lu, H. Kono, T. I. Larkin, A. W. Rost, T. Takayama, A. V. Boris, B. Keimer, and H. Takagi, Zero-gap semiconductor to excitonic insulator transition in Ta_2NiSe_5, Nat. Commun. **8**, 14408 (2017).

[10] T. I. Larkin, A. N. Yaresko, D. Propper, K. A. Kikoin, Y. F. Lu, T. Takayama, Y.-L. Mathis, A. W. Rost, H. Takagi, B. Keimer, and A. V. Boris, Giant exciton Fano resonance in quasi-one-dimensional Ta_2NiSe_5, Phys. Rev. B **95**, 195144 (2017).

[11] K. Sugimoto, S. Nishimoto, T. Kaneko, and Y. Ohta, Strong Coupling Nature of the Excitonic Insulator State in Ta_2NiSe_5, Phys. Rev. Lett. **120**, 247602 (2018).

[12] S. Mor, M. Herzog, D. Golez, P. Werner, M. Eckstein, N. Katayama, M. Nohara, H. Takagi, T. Mizokawa, C. Monney, and J. Stähler, Ultrafast Electronic Band Gap Control in an Excitonic Insulator, Phys. Rev. Lett. **119**, 086401 (2017).

[13] K. Okazaki, Y. Ogawa, T. Suzuki, T. Yamamoto, T. Someya, S. Michimae, M. Watanabe, Y. Lu, M. Nohara, H. Takagi, N. Katayama, H. Sawa, M. Fujisawa, T. Kanai, N. Ishii, J. Itatani, T. Mizokawa, and S. Shin, Photo-induced semimetallic states realised in electron-hole coupled insulators, Nat. Commun. **9**, 4322 (2018).

[14] T. Mitsuoka, T. Suzuki, H. Takagi, N. Katayama, H. Sawa, M. Nohara, M. Watanabe, J. Xu, Q. Ren, M. Fujisawa, T. Kanai, J. Itatani, S. Shin, K. Okazaki, and T. Mizokawa, Photoinduced phase transition from excitonic insulator to semimetal-like state in $Ta_2Ni_{1-x}Co_xSe_5$ ($x = 0.10$), J. Phys. Soc. Jpn. **89**, 124703 (2020).

[15] T. Tang, H. Wang, S. Duan, Y. Yang, C. Huang, Y. Guo, D. Qian, and W. Zhang, Non-Coulomb strong electron-hole binding in Ta_2NiSe_5 revealed by time- and angle-resolved photoemission spectroscopy, Phys. Rev. B **101**, 235148 (2020).

[16] T. Suzuki, Y. Shinohara, Y. Lu, M. Watanabe, J. Xu, K. Ishikawa, H. Takagi, M. Nohara, N. Katayama, H. Sawa, M. Fujisawa, T. Kanai, J. Itatani, T. Mizokawa, S. Shin, and K. Okazaki, Detecting electron-phonon coupling during photoinduced phase transition, Phys. Rev. B **103**, L121105 (2021).

[17] T. Saha, D. Golez, G. De Ninno, J. Mravlje, Y. Murakami, B. Ressel, M. Stupar, and P. R. Ribic, Photoinduced phase transition and associated timescales in the excitonic insulator Ta_2NiSe_5, Phys. Rev. B **103**, 144304 (2021).

[18] K. Fukutani, R. Stania, J. Jung, E. F. Schwier, K. Shimada, C. I. Kwon, J. S. Kim, and H. W. Yeom, Electrical Tuning of the Excitonic Insulator Ground State of Ta_2NiSe_5, Phys. Rev. Lett. **123**, 206401 (2019).

[19] L. Chen, T. T. Han, C. Cai, Z. G. Wang, Y. D. Wang, Z. M. Xin, and Y. Zhang, Doping-controlled transition from excitonic insulator to semimetal in Ta_2NiSe_5, Phys. Rev. B **102**, 161116(R) (2020).

[20] M. D. Watson, I. Markovic, E. A. Morales, P. Le Fevre, M. Merz, A. A. Haghighirad, and P. D. C. King, Band hybridization at the semimetal-semiconductor transition of Ta_2NiSe_5 enabled by mirror-symmetry breaking, Phys. Rev. Res. **2**, 013236 (2020).

[21] K. Fukutani, R. Stania, C. I. Kwon, J. S. Kim, K. J. Kong, J. Kim, and H. W. Yeom, Detecting photoelectrons from spontaneously formed excitons, Nat. Phys. **17**, 1024 (2021).

[22] Y.-S. Seo, M. J. Eom, J. S. Kim, C.-J. Kang, B. I. Min, and J. Hwang, Temperature-dependent excitonic superfluid plasma frequency evolution in an excitonic insulator Ta_2NiSe_5, Sci. Rep. **8**, 11961 (2018).

[23] K. Matsubayashi, H. Okamura, T. Mizokawa, N. Katayama, A. Nakano, H. Sawa, T. Kaneko, T. Toriyama, T. Konishi, Y. Ohta, H. Arima, R. Yamanaka, A. Hisada, T. Okada, Y. Ikemoto, T. Moriwaki, K. Munakata, A. Nakao, M. Nohara, Y. Lu *et al.*, Hybridization-gap formation and superconductivity in the pressure-induced semimetallic phase of the excitonic insulator Ta_2NiSe_5, J. Phys. Soc. Jpn. **90**, 074706 (2021).

[24] J. Yan, R. Xiao, X. Luo, H. Lv, R. Zhang, Y. Sun, P. Tong, W. Lu, W. Song, X. Zhu, and Y. Sun, Strong electron-phonon coupling in the excitonic insulator Ta_2NiSe_5, Inorg. Chem. **58**, 9036 (2019).

[25] M.-J. Kim, A. Schulz, T. Takayama, M. Isobe, H. Takagi, and S. Kaiser, Phononic soft mode behavior and a strong electronic background across the structural phase transition in Ta_2NiSe_5, Phys. Rev. Res. **2**, 042039(R) (2020).

[26] S. Pal, S. Grover, L. Harnagea, P. Telang, A. Singh, D. V. S. Muthu, U. V. Waghmare, and A. K. Sood, Destabilizing excitonic insulator phase by pressure tuning of exciton-phonon coupling, Phys. Rev. Res. **2**, 043182 (2020).

[27] K. Kim, H. Kim, J. Kim, C. Kwon, J. S. Kim, and B. J. Kim, Direct observation of excitonic instability in Ta_2NiSe_5, Nat. Commun. **12**, 1969 (2021).

[28] P. A. Volkov, M. Ye, H. Hohani, I. Feldman, A. Kanigel, and G. Blumberg, Critical charge fluctuations and emergent coherence in a strongly correlated excitonic insulator, npj Quantum Mater. **6**, 52 (2021).

[29] D. Werdehausen, T. Takayama, M. Höppner, G. Albrecht, A. W. Rost, Y. Lu, D. Manske, H. Takagi, and S. Kaiser, Coherent order parameter oscillations in the ground state of the excitonic insulator Ta_2NiSe_5, Sci. Adv. **4**, eaap8652 (2018).

[30] S. Mor, M. Herzog, J. Noack, N. Katayama, M. Nohara, H. Takagi, A. Trunschke, T. Mizokawa, C. Monney, and J. Sähler, Inhibition of the photoinduced structural phase transition in the excitonic insulator Ta_2NiSe_5, Phys. Rev. B **97**, 115154 (2018).

[31] T. Miyamoto, M. Mizui, N. Takamura, J. Hirata, H. Yamakawa, T. Morimoto, T. Terashige, N. Kida, A. Nakano, H. Sawa, and H. Okamoto, Charge and lattice dynamics in excitonic insulator Ta_2NiSe_5 investigated using ultrafast reflection spectroscopy, J. Phys. Soc. Jpn. **91**, 023701 (2022).

[32] C. Monney, M. Herzog, A. Pulkkinen, Y. Huang, J. Pelliciari, P. Olade-Velasco, N. Katayama, M. Nohara, H. Takagi, T. Schimitt, and T. Mizokawa, Mapping the unoccupied state dispersions in Ta_2NiSe_5 with resonant inelastic x-ray scattering, Phys. Rev. B **102**, 085148 (2020).

[33] H. Lu, M. Rossi, J.-H. Kim, H. Yavas, A. Said, A. Nag, M. Garcia-Fernandez, S. Agrestini, K.-J. Zhou, C. Jia, B. Moritz, T. P. Devereaux, Z.-X. Shen, and W.-S. Lee, Evolution of the electronic structure in Ta_2NiSe_5 across the structural transition revealed by resonant inelastic x-ray scattering, Phys. Rev. B **103**, 235159 (2021).

[34] A. Nakano, K. Sugawara, S. Tamura, N. Katayama, K. Matsubayashi, T. Okada, Y. Uwatoko, K. Munakata, A. Nakao, H. Sagayama, R. Kumai, K. Sugimoto, N. Maejima, A. Machida, T. Watanuki, and H. Sawa, Pressure-induced coherent sliding-layer transition in the excitonic insulator Ta_2NiSe_5, IUCrJ **5**, 158 (2018).

[35] J. Lee, C.-J. Kang, M. J. Eom, J. S. Kim, B. I. Min, and H. W. Yeom, Strong interband interaction in the excitonic insulator phase of Ta_2NiSe_5, Phys. Rev. B **99**, 075408 (2019).

[36] A. Subedi, Orthorhombic-to-monoclinic transition in Ta_2NiSe_5 due to a zone-center optical phonon instability, Phys. Rev. Mater. **4**, 083601 (2020).

[37] G. Mazza, M. Rösner, L. Windgätter, S. Latini, H. Hübener, A. J. Millis, A. Rubio, and A. Georges, Nature of Symmetry Breaking at the Excitonic Insulator Transition: Ta_2NiSe_5, Phys. Rev. Lett. **124**, 197601 (2020).

[38] See Supplemental Material at http://link.aps.org/supplemental/10.1103/PhysRevB.107.045141 for the optical spectra measured at $P = 0$ and the Raman data measured at high P.

[39] H. Okamura, Y. Ikemoto, T. Mariwaki, and T. Nanba, Infrared spectroscopy techniques for studying the electronic structures of materials under high pressure, Jpn. J. Appl. Phys. **56**, 05FA11 (2017).

[40] G. J. Piermarini, S. Block, J. D. Barnett, and R. A. Forman, Calibration of the pressure dependence of the R_1 ruby fluorescence line to 195 kbar, J. Appl. Phys. **46**, 2774 (1975).

[41] S. Kimura and H. Okamura, Infrared and terahertz spectroscopy of strongly correlated electron systems under extreme conditions, J. Phys. Soc. Jpn. **82**, 021004 (2013).

[42] T. Moriwaki and Y. Ikemoto, BL43IR at SPring-8 redirected, Infrared Phys. Tech. **51**, 400 (2008).

[43] M. Dressel and G. Grüner, *Electrodynamics of Solids* (Cambridge University Press, Cambridge, 2002).

[44] H. Okamura, A simple method for the Kramers-Kronig analysis of reflectance spectra measured with diamond anvil cell, J. Phys.: Conf. Ser. **359**, 012013 (2012).

[45] H. Okamura, Methods for obtaining the optical constants of a material, *Optical Techniques for Solid State Materials Characterization*, edited by R. Prasankumar and A. Taylor (CRC, Boca Raton, FL, 2011), Chap. 4.

[46] D. N. Basov, R. D. Averitt, D. van der Marel, M. Dressel, and K. Haule, Electrodynamics of correlated electron materials, Rev. Mod. Phys. **83**, 471 (2011).

[47] The volume per f.u. at room temperature and $P = 0$, 2.5, 3.5, and 6.5 GPa have been estimated to be 173, 165, 159, and 150 Å^3, respectively, from the crystal structure data at high P [34]. In the calculation of $N^*(\omega)$, the volume contraction with cooling has been neglected, since it is much smaller than that with increasing P.

[48] J. J. Wu, J.-F. Lin, X. C. Wang, Q. Q. Liu, J. L. Zhu, Y. M. Xiao, P. Chow, and C. Jin, Pressure-decoupled magnetic and structural transitions of the parent compound of iron-based 122 superconductors $BaFe_2As_2$, Proc. Natl. Acad. Sci. USA **110**, 17263 (2013).